



Chitosan Based Polyelectrolyte Complexes Development For Anionic And Cationic Dyes Adsorption



Eman A. Ali¹, Mohamed N. Ismail*¹, Maher Z. Elsabee²

¹Polymers and Pigments Department, National Research Centre, 12622 Dokki, and

²Chemistry Department, Faculty of Science, Cairo University, 12613 Giza, Egypt

A huge amounts of hazardous dyes from different industries are causing water pollution, the removal of these compounds from a process or waste effluents becomes a crucial environmental importance. The adsorption method has been found to handle large quantities without the formation of hazardous substances. In spite of the efficiency of the adsorption technique, the high cost of the adsorbent materials is a stumbling block for large scale applications. An eco-friendly, low-cost and efficient adsorbent has been prepared for wastewater management. Hydrolyzed and sulphonated styrene maleic anhydride copolymers, were mixed with chitosan to form nano-polyelectrolyte complexes. Structure, particle size and thermal behavior of the complexes were investigated by spectral and thermogravimetric analyses. The hydrolyzed and sulphonated styrene maleic anhydride chitosan complexes (H-SMA-CS and S-SMA-CS) were examined for the adsorption of Congo red and Maxilon blue as anionic and cationic dyes, respectively. The experimental data of adsorption were found to fit the pseudo-second-order kinetic. The maximum adsorption capacities of Congo red were 234 and 116 mg/g where those of Maxilon blue were 702 and 1830 mg/g on S-SMA-CS and H-SMA-CS, respectively. The isotherm results were well fitted by the Freundlich isotherm.

Keywords: Chitosan, Styrene maleic anhydride, Polyelectrolyte complexes, Congo red, Maxilon blue, Isotherm, Kinetics

Introduction

In the history of mankind, no century possibly witnessed an increased interest in wastewater treatment than this century for tolerating industrial development. One of the challenging issues is dealing with dyes. As huge amounts of hazardous dyes from the textile, printing, paper, cosmetic, plastic and food industry wastes are dumped into the water causing the damage of the environment. Since a very small amount of dye in water is highly treacherous as it is toxic to creatures in water, the removal of these compounds from a process or waste effluents becomes a crucially environmental importance. In addition, the complex aromatic structure of commonly used dyes resists biodegradation or photo degradation[1]. Congo red (CR) and Maxilon blue (MB) are dyes which

are regarded as hazardous chemicals. Congo red (CR), a known anionic dye, is metabolized to benzidine which is a famous carcinogen. Thus its introduction to water stream is a potential health, environmental, and ecological concern. Therefore, a dye containing effluents has to be sufficiently treated before they are discharged into the water system[2]. Adsorption of dyes from aqueous solutions proved to be the most efficient technique for wastewater treatment [3] compared with other conventional techniques such as coagulation, precipitation, filtration, ozonation, reverse osmosis and oxidation[4–6]. The adsorption method[7, 8] has been found to handle large quantities without the formation of hazardous substances such as the free radicals. In spite of the efficiency of the adsorption

* Corresponding author: naderdiab2003@yahoo.com

Received 4/12/2019, accepted 20/1/2020

DOI: 10.21608/ejchem.2020.20522.2229

©2020 National Information and Documentation Center (NIDOC)

technique, the high cost of the adsorbent materials is a stumbling block for large scale applications. Therefore researchers enthusiastically tried to find cheap and abundant materials to be applied for the removal of dyes[9–12]. By combining different materials as well as using diverging methods,[13, 14] the cost and efficiency of the dye uptake will be improved.

Chitosan (CS) a derivative of natural and abundant polymer chitin, was found to have a high impact in adsorption of anionic dyes[15]as well as in many applications[16–18]. Chitosan efficiency for the removal of dyes in aqueous solutions have been reported [19, 20] whether by grafting with a polymer containing useful functional groups [21, 22] or by blending with functional polymers[23, 24]. Many attempts have been employed to extend the efficiency of chitosan to adsorb the cationic dyes through composite preparation[6] and working in the frame of low-cost modification is still of great interest.

Styrene maleic anhydride (SMA) is a conversant copolymer since it is easily prepared from two inexpensive monomers in addition to the presence of a very reactive anhydride group which can easily react with a multiple of functional groups to form many derivatives[25–29]. SMA and its derivatives have been comprehensively used in many industrial [30]and medical applications[31–33]. It has also been used for dyes adsorption, for example, Zhang, et al, modified SMA by β -cyclodextrin through grafting and acylation and for the removal of methylene blue and basic fuchsin[34]. Sulphonated SMA microspheres were prepared and investigated as an adsorbent of methylene blue and rhodamine and was found to have an exceptional adsorption capacity[35]. In a like manner, SMA was grafted on alginate hydrogel [36]. It was described by Eskhan, et al, to have a Langmuir adsorption for methyl violet 6B.

For the sake of efficient along with commercial adsorbent, it was aimed in this work to adopt the nanotechnology for exaggerating the benefits of these two abundant, biocompatible, and low-cost polymers for dye adsorption. The present work describes the preparation and characterization of polyelectrolyte complex (PEC) nanoparticles through the electrostatic interaction between the oppositely charged polyelectrolyte SMA derivatives and chitosan. The immediate production of PECs without the addition of chemical crosslinking reagent reduce the cost as

well as the toxicity of the prepared materials. In addition, as most PECs, they have the strongest physical interaction due to their preparation high entropy as a result of the release of the low molar counter ion[37]. Herein, the prepared PECs were not previously reported for dye removal. This study investigates the adsorption efficiency of chitosan /hydrolyzed and sulphonated styrene maleic anhydride copolymer complexes for the removal of anionic and cationic dyes.

Experimental

Materials

Styrene was a product of Aldrich. Maleic anhydride (99% Merck) was recrystallized from chloroform prior to use, Benzoyl peroxide (BPO), a Merck product, was re-crystallized from methanol. Chloro sulphonic acid (Merck), hydrochloric acid (HCl), and sulfuric acid (H_2SO_4) were reagent grade and used as received. Potassium chloride (KCl), potassium permanganate ($KMnO_4$) and sodium hydroxide (NaOH) were obtained from the local company(ADWIEK). Congo red (CR) and Maxilon blue (MB) were products of a local company. Acetone, acetic acid, ethylene chloride, methanol and toluene were used as received.

Chitosan extraction

Chitin was extracted from red sea marine shrimp, washed with water, dried, and grinded into grainy powder. First, the powder was soaked in 1 M hydrochloric acid, HCl, bathes for the removal of $CaCO_3$. Afterwards, the alkaline treatment used 1 M sodium hydroxide (NaOH) solutions at 105-110°C was performed for the removal of protein. This treatment was repeated till almost the occurrence of clear medium. After filtration, washing with a massive amount of distilled water are required after which the samples were dried. Pigments were removed by using a mild oxidizing treatment ($KMnO_4$ + oxalic acid + H_2SO_4). By boiling the isolated chitin with 40%NaOH, deacetylation was carried out according to reference[38].

Determination of the degree of deacetylation (DDA):

Two methods have been used to calculate the DDA% of chitosan by elemental analysis and potentiometric titration according to literature reported methods[39, 40].

Viscosity:

Using Ostwald viscometer, the intrinsic viscosity of the extracted chitosan was determined. A solution of 5% acetic acid containing 0.2 M

sodium chloride to overpower the charges effect of the amino groups was used as a solvent for chitosan. The intrinsic viscosity $[\eta]$ molecular weight equation of Mark-Houwink molecular weight [41] was implemented for the calculation of the molecular weight.

$$([\eta] = k M^a).$$

Synthesis of (styrene-alt-maleic anhydride)

Using a free-radical polymerization, SMA was prepared [42] in a 500 mL four-necked flask, with magnetic stirrer, thermometer, reflux condenser and inlet of nitrogen 10.4 g of destabilized styrene, 9.8 g of recrystallized maleic anhydride, and 0.2 g (0.8 mmole) of BPO were mixed with 200 ml of distilled toluene at room temperature until a clear solution was obtained. The reaction mixture was continuously stirred and heated to 80°C on a water bath, the copolymer gradually precipitated, after 3 h the mixture was cooled, the filtration of the white solid polymer was carried out and was dried to constant weight under vacuum at 60°C. SMA was re-precipitated in methanol from acetone.

Synthesis of sulphonated (styrene-alt-maleic anhydride)

0.37 moles of SMA were suspended in 480 mL of ethylene dichloride. Then 0.28 moles of chlorosulfonic acid dissolved in 50 mL of ethylene dichloride were gradually added. To this well agitated mixture no cooling or heating is required;

the temperature remained for one and half hour after the chlorosulfonic acid complete addition at about 34° C. The product was then removed by filtration and was air-dried to yield 0.4 mole of a light tan solid[43].

Synthesis of hydrolyzed styrene-alt-maleic anhydride

Hydrolysis of SMA was performed in alkaline aqueous solution. Using 100 mL of 1 N NaOH solution, a complete dissolution of SMA (2 g) took place. Then, precipitation was carried out by adding 1 N HCl drop wise to get a white precipitate after which the hydrolyzed-SMA (H-SMA) was formed. The washing with minimum amount of water to neutralize the acid was performed. After that, it was kept in oven for 24 h[44].

Preparation of styrene-maleic anhydride derivatives/chitosan nanopolyelectrolyte complexes

An aqueous solution of sodium salt of hydrolyzed copolymer of SMA (pH 4.0) or sulphonated SMA (pH 5.5) was added to a certain amount (20 mL) of 2% CS solution. The polyelectrolyte complexes formation was indicated by a precipitate occurrence as a result of mixing as shown in Fig. 1. By centrifugation at 5 000 rpm for 20 min, the separation was achieved. Then, the product was washed with water and acetone. The precipitate was dried under vacuum till constant weight and then grinded into fine particles.

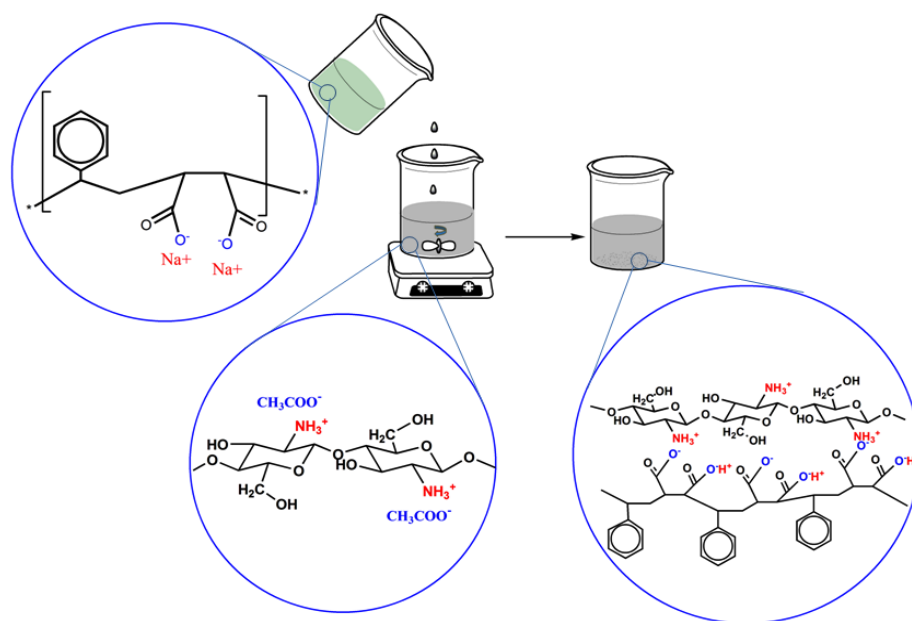


Fig.1 Schematic representation of the preparation of polyelectrolyte of hydrolyzed SMA-CS complexes

Dye Uptake

The adsorption process was performed using a batch adsorption technique at $25^{\circ}\text{C} \pm 2$. The samples (0.005 g) were held in 10 ml of the dyes (Congo red as acidic dye and Maxilon blue as a basic dye) solution in 120 rpm shaker for a certain time. The UV-visible spectra were then measured at wavelength 497 and 602 nm for Congo red (CR) and Maxilon blue (MB), respectively. **Figure (2)** shows the structure of the examined dyes.

Characterization

FTIR Spectroscopy

FTIR spectra were measured at a resolution of 4 cm^{-1} . The range of measurement was 400 to 4000 cm^{-1} Using spectrometer Bruker Vector 22 Germany.

Thermal Analysis

Thermogravimetric TGA analysis was accomplished at a heating rate of $10^{\circ}\text{C}/\text{min}$ under nitrogen atmosphere by Shimadzu TGA-50H.

Dynamic Light Scattering (DLS)

Zetasizer, Nano-S, produced by Malvern, was the instrument used for measuring the particles size. DLS was used to measure the hydrodynamic diameter and size distribution of the particles at 25°C in triplicate considering the refractive index of 1.52.

Scanning Electron Microscopy (SEM)

Jeol JSM 6610 microscope was used for studying the particle morphology at the accelerating voltage of 15 kV. A thin layer of gold was used as a coating. The micrographs

processing was achieved with AzTec software.

The UV-visible Spectroscopy

The UV-visible spectra of the samples were then measured using Agintal UV-visible spectrophotometer (USA).

Results and Discussions

Chitosan

Determination of the degree of deacetylation of chitosan (DDA %)

Several methods are known for the determination of DDA %, among the simplest and quite reliable are the following:

Elemental analysis:

From the elemental analysis data: C% 39.17, H% 7.24, and N% 7.46 and using the formula:

$$DDA\% = \frac{6.857 - C/N}{1.7143} \times 100 \quad (3.1)$$

The value of the DDA for chitosan is found to be = 93.7%.

Potentiometric titration:

From the acid/base titration curve two inflection points were obtained. These inflection points were attributed to the NaOH volume corresponding to the amino group of chitosan.

Therefore, the DDA can be calculated by the following formula [38]

$$DDA\% = \frac{1 - 161Q}{1 + 2Q} \times 100 \quad (3.2)$$

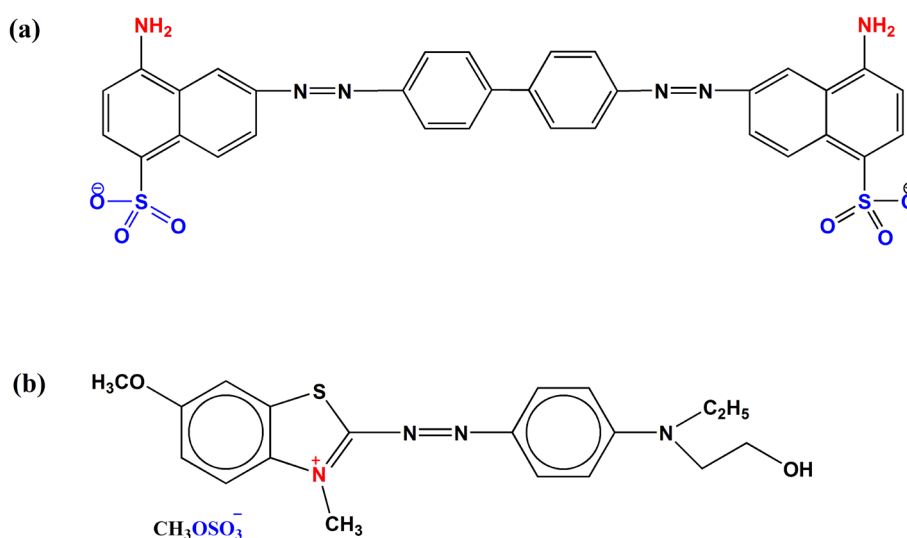


Fig.2. Chemical structure of (a) Congo red and (b) Maxilon blue

Where $Q = N \Delta v/m$, Δv is the volume of NaOH between the two inflection points (in l liter), N is the normality of the sodium hydroxide and m is the weight of the dry sample. $\Delta v = 8$ ml and a value of 94.09 % was obtained for the DDA by this method.

FTIR analysis:

Figure 3 (f) shows, the characteristic, broadband around 3400 cm^{-1} which is due to the inter- and intra-molecular interaction between the OH and the NH₂ groups stretching vibration of the chitosan unit. The 2920.66 and 2365.22 cm^{-1} bands are due to the asymmetric and symmetric C-H stretching of the methylene groups in the residual chitin molecules. The bands at 1650.01 cm^{-1} is due to the amide I (C=O stretching) and that at 1603 cm^{-1} is probably due to the amide II (N-H stretching).

Molecular weight

The viscosity average molecular weight M_v of chitosan was estimated by applying the following Mark-Houwink equation ($[\eta] = k M_v^a$) for chitosan. Where k (6.896×10^{-3}) and a (0.86) are constants depending on the specific polymer-solvent-temperature system and the degree of deacetylation of chitosan [45]

$$[\eta] = 6.896 \times 10^{-3} M_v^{0.86} \quad (3.3)$$

The intrinsic viscosity ($[\eta]$) was determined from viscosity measurements using Ostwald viscometer. A value of 25.72 was found for $[\eta]$ dL/g which corresponds to relatively low molecular weight chitosan of 1.4×10^4 g/mol.

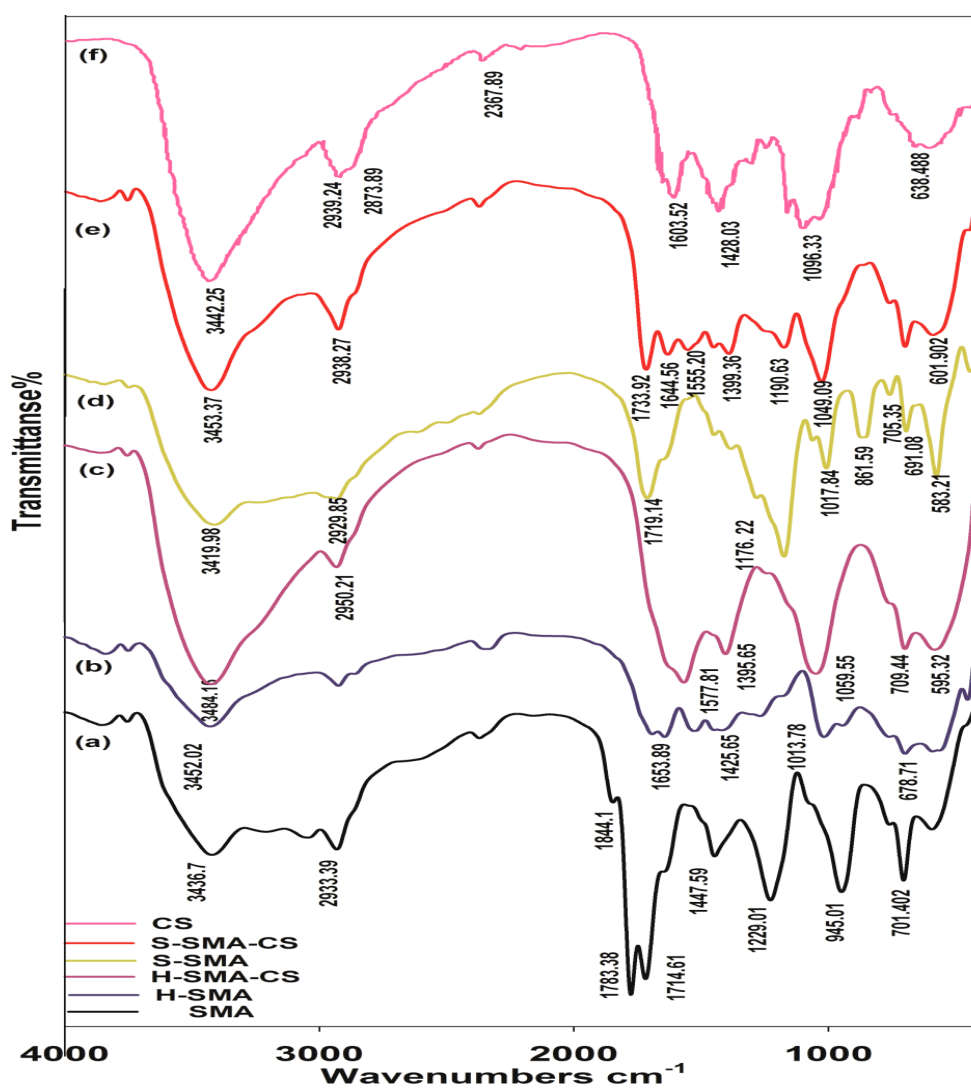


Fig. 3. FTIR spectra of (a)SMA, (b)hydrolyzed SMA, (c) hydrolyzed SMA-CS, (d)sulphonated SMA, (e) sulphonated SMA-CS, and (f)chitosan (CS).

Styrene-alt-maleic anhydride (SMA) and its derivatives

FTIR analysis

The spectra of SMA and its derivatives are shown Fig.3. Peaks at 1844.1 and 1780 cm^{-1} imply the presence of anhydride groups resulting from the carbonyl absorption in the five-membered rings. In the case of hydrolysed copolymer H-SMA, the C=O band disappears, being replaced by the carboxyl band at 1735 cm^{-1} . Introduction of the sulfonic acid groups is confirmed by the strong characteristic peak at 1176.22 cm^{-1} which is assigned to the stretching of S=O bond. The characteristic absorption peaks at 1176.22 and 1017.84 cm^{-1} correspond to the asymmetric S=O and symmetric O=S=O stretching vibrations of the sulfonate groups, respectively. The two peaks at 705.35 and 691.08 cm^{-1} are considered relate to the C-S and S-OH stretching vibration, which were reported to lie between 600 and 800 cm^{-1} and 600 and 700 cm^{-1} , respectively.

Molecular weight:

The molecular weight of SMA can be determined from the viscosity measurements by using the Mark-Houwink equation of its acetone solution according to the following equation from the reference[46]

$$\eta = 8.69 \times 10^{-5} M_p^{0.74} \quad (3.4)$$

The intrinsic viscosity $[\eta]$ was found to be 1.19 dl/g.

Particle size

Particle size measurements using DLS measurements shown in **Figure 4**, indicates that SMA was formed in micro-particles with a size of 1.35 μm .

Polyelectrolyte complexes of styrene-maleic anhydride /chitosan

FTIR analysis

The IR-spectra of SMA and chitosan and the complexes showed a new zone of absorption in the region of 1577–1507 cm^{-1} that corresponds to the symmetrical deformational vibrations of NH_3^+ groups. The strong bands of absorption in the regions of 1577–1551 cm^{-1} (symmetrical vibrations of COO^-) and 1408–1395 cm^{-1} (asymmetrical vibrations of COO^-) as observed in Fig.3 confirm the formation of ionic polyelectrolyte complexes H-SMA-CS. The spectrum of the complex in **Figure 3** (e) showed that the band at 1603 cm^{-1} shifted to 1529 cm^{-1} , while the characteristic band for S-SMA in the

region of 1719–1733 cm^{-1} remained is a clear evidence of both polymers contribution in the final polyelectrolyte complex composition.

Particle size

Utilizing dynamic light scattering investigation, as shown in Fig.4, reveals average particle diameters of 423 ± 0.01 nm with a poly dispersity index (PDI) of 0.5 ± 0.05 for H-SMA-CS, and 105 ± 1 nm with PDI: $1 \pm$ for S-SMA-CS. The zeta potential (mV) equal -11. and 9.8 for S-SMA-CS and H-SMA-CS, respectively.

Morphology of the polyelectrolyte complexes

As shown in **Figure 4** (d) and (e) there is an obvious dissimilarity in the morphology between the two polyelectrolytes complexes. A layered structure, the ladder like structure, is observed for H-SMA-CS, whereas S-SMA-CS image shows a semi-spherical spongy structure, the scrambled egg structure. The highly order arrangement of HSMA-CS is due to the interaction between one hydrophilic group with more than on hydrophobic moiety(styrene); it can be described as zippering effect where the ionic sites interact with each other one by one[37]. The scrambled egg structure is significance for stoichiometry polyelectrolyte complexes where polyions chains are 1:1. This morphology of the macrostructure of the two PECs is likely to have an impact of the adsorption behaviour and mechanism of diffusion.

Thermogravimetric analysis

Figure 5 illustrates the TGA of SMA, hydrolyzed SMA (H-SMA), sulfonated SMA (S-SMA), chitosan (CS) and poly electrolyte complexes of chitosan and SMA derivatives (H-SMA-CS) and (S-SMA-CS), it can be seen that CS is the least thermal stable polymer and the SMA is the highest thermally stable one. Mixing CS with H-SMA gives a moderately stable PEC indicating a synergetic effect due to the strong electrostatic attraction between the NH_2 of CS and the multiple functional groups OH and COOH formed after the hydrolysis of SMA copolymer. Three weight loss stages can be clearly shown for (S-SMA). The first occurs at 35–100°C which is attributed to the loss of water as S-SMA has a hygroscopic nature. The second occurs in the range of 150–225°C the weight loss associated with the elimination of the sulfonic groups. The last loss stage at 350–500°C is the final decomposition of S-SMA. A summary of the TGA data is compiled in **Table 1**. Admittedly, not only the strong electrostatic interaction between CS and the two derivatives of SMA afforded the

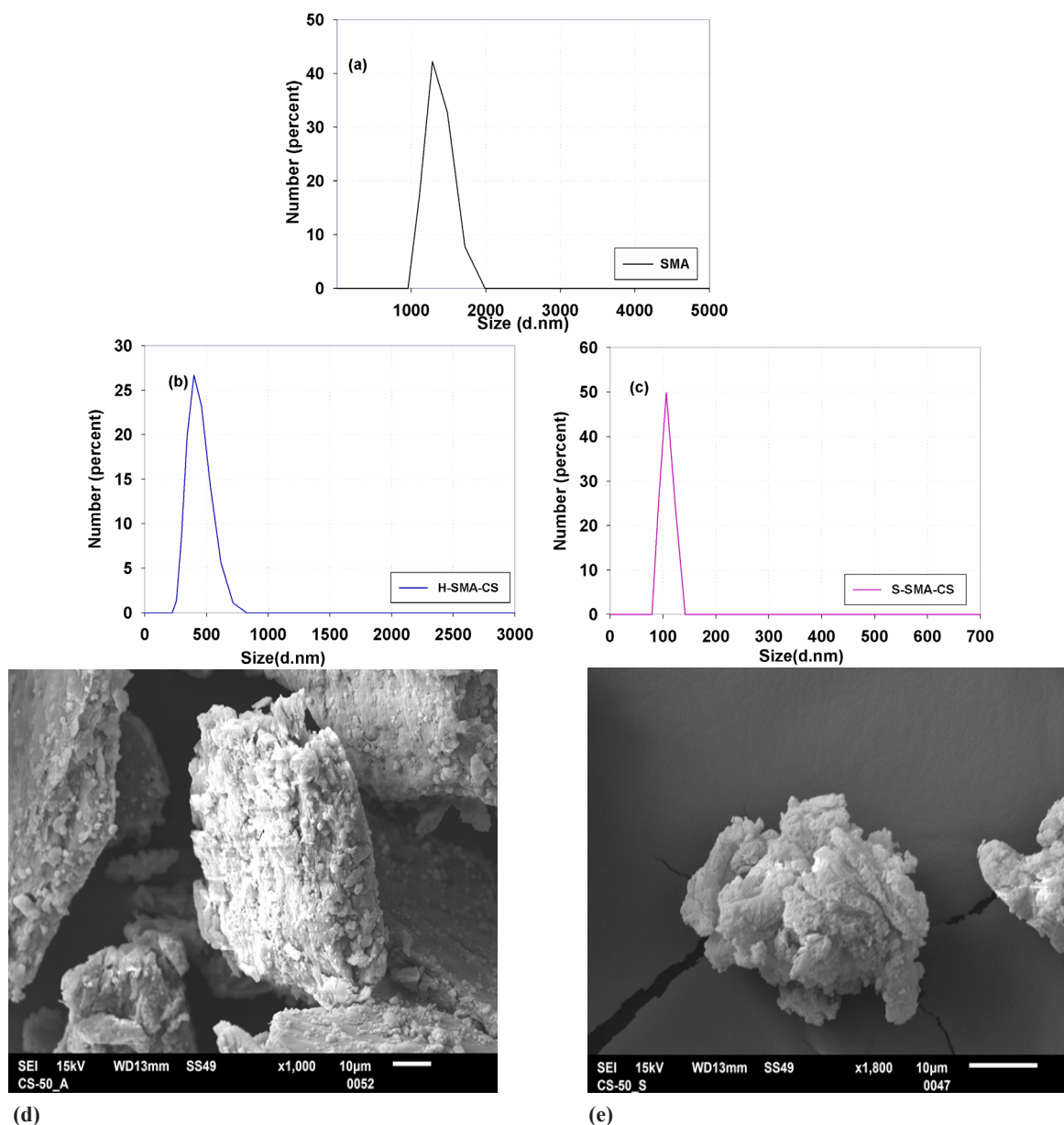


Fig. 4. Size distribution of (a) SMA microparticles, (b) hydrolyzed SMA-CS, and (c) sulphonated SMA-CS nanoparticles and SEM images of (d)H-SMA-CS and (e) S-SMA-CS

high thermal stability of the two PECs but also to the hydrogen bonding and the hydrophobic interaction.

Dye uptake

Effect of pH

The adsorption capacity was calculated for the adsorption of 75 ppm of CR and MB on 0.005 g of the two composites. The variation of the medium acidity or basicity has its role in the adsorption process. **Figure 6** shows the behavior of the adsorbent at different pH values. Generally, zeta potential is known to be increased by decreasing

pH [6] as a result of the protonation of the freely amino group of chitosan. Consequentially the pH increasing will lead to the deprotonation of carboxylic and sulfonate groups on SMA-CS composite and the neutralization of amino group on the surface of the adsorbent. By increasing the pH, the CR adsorption increased. This behavior is attributed to the increase of the electrostatic attraction between the positively charged dye and the deprotonated carboxylate and sulfonate groups. Regarding the MB, slightly acidic medium enhanced the adsorption on both S-SMA-

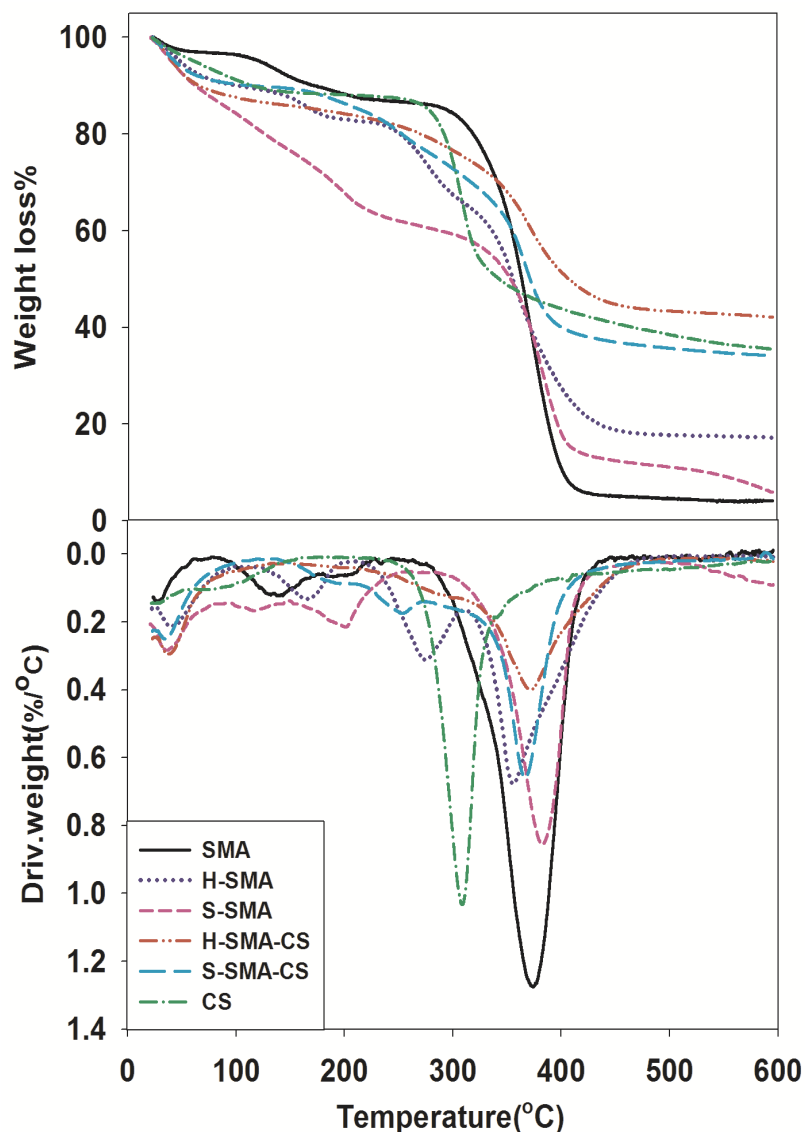


Fig.5. Thermogravimetric analysis of SMA, hydrolyzed SMA, sulphonated SMA, hydrolyzed SMA-CS polyelectrolyte complexes, sulphonated SMA-CS polyelectrolyte complexes and chitosan

TABLE 1. Thermogravimetric analysis data of the samples

Sample	T _{initial}	T _{final}	T _{max}	Wt loss%	Remaining wt.% at 600°C
SMA	279.00	400.00	374.00	96.00	4.13
H-SMA	106.00	596.00	355.00	82.80	17.20
S-SMA	198.00	596.00	382.00	91.70	8.13
H-SMA-CS	172.00	431.00	372.00	46.60	42.10
S-SMA-CS	216.00	596.00	367.00	65.70	34.30
CS	273.00	331.00	308.00	64.40	35.60

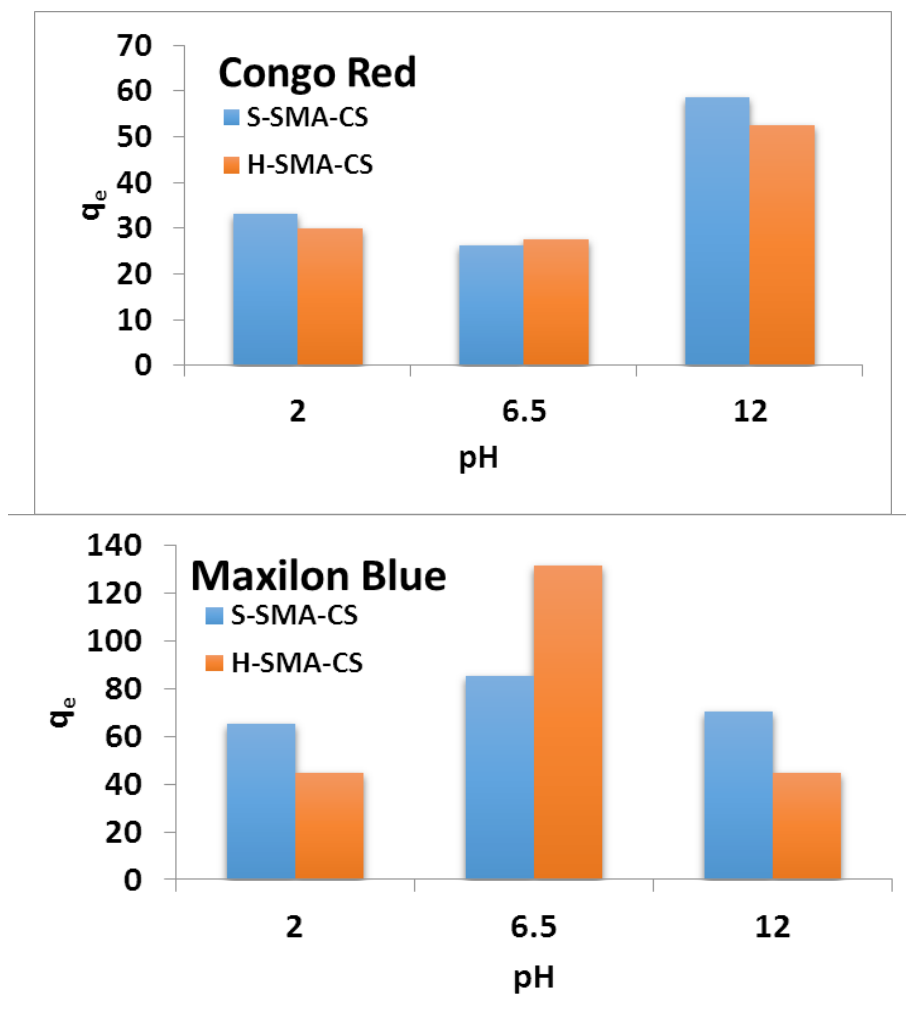


Fig.6. Effect of pH on the adsorption capacity of S-SMA-CS and H-SMA-CS

CS and H-SMA-CS. It is clear that the difference is correlated to the change of the surface charge.

Adsorption kinetics

The efficiency of adsorption process is controlled by the way of the dye transition which is generally, affected by the adsorbent surface characteristics. Therefore, investigating adsorption process according to kinetic models helps to evaluate the appropriate adsorbent for dye removal with time.

The modeling of the kinetics of adsorption of Congo red and Maxilon blue was investigated by two common models, namely, the Lagergren pseudo-first-order model and pseudo-second-order model. Equation of the pseudo-first-order was examined to study the adsorption kinetics.

$$\log(q_e - q_t) = \log q_e - \frac{k_t}{2.303} t \quad (3.5)$$

Where, q_e (mg/g) is the concentration of the ion adsorbed at equilibrium, q_t (mg/g) is the concentration of the ion adsorbed at time t , and k is the rate constant. The equation below signifies another kinetic model, the pseudo-second-order,

$$\frac{t}{q_t} = \frac{1}{k_2 q_e^2} + \frac{1}{q_e} t \quad (3.6)$$

From the slope or the intercept of the straight line in **Figure 7** and **Figure 8** the adsorbed amount of dye at equilibrium (q_e), the adsorption rate constant (k_1) of "pseudo- first order", and adsorption rate constant (k_2) of pseudo - second order can be calculated. The fitness of the straight lines (R^2 values) with the linear forms of the models is evaluated to check the applicability of each model.

The data in **Table 2**, indicate the disagreement of this model, the Lagergren pseudo-first-order

kinetic, with the adsorption of both dyes, on the two polyelectrolytes complexes. On the contrary, the experimental data as indicated from the high values of the correlation coefficient R^2 (for Congo red $R^2 \geq 0.98$ and $R^2 \geq 0.99$ for S-SMA-CS and H-SMA-CS, respectively, and for Maxilon blue $R^2 \geq 0.89$ and $R^2 \geq 0.99$ for S-SMA-CS and H-SMA-CS, respectively) was found to best fit the pseudo-second-order kinetic. So, the pseudo-second-order kinetic model can be applied to anticipate the dye uptake at equilibrium at different contact time intervals.

There are two ways to describe adsorption rate either by intra-particle diffusion or boundary layer

diffusion or both. Therefore, The model based on the Weber and Morris theory for intra-particle diffusion [26] was tested. According to this theory:

$$q_t = k_p t^{1/2} + C_i \quad (3.7)$$

Where k_{pi} ($\text{mg/g min}^{1/2}$), the rate parameter of stage i , is calculated from the slope of the straight line of q_t versus $t^{1/2}$ (Fig.9) The values of k_{pi} , C_i and correlation coefficient, R^2 obtained for the plots are given in Table3

There are three phases, in Figure 9, obtained for Congo red adsorption in "Weber and Morris" intra-particle diffusion plots.

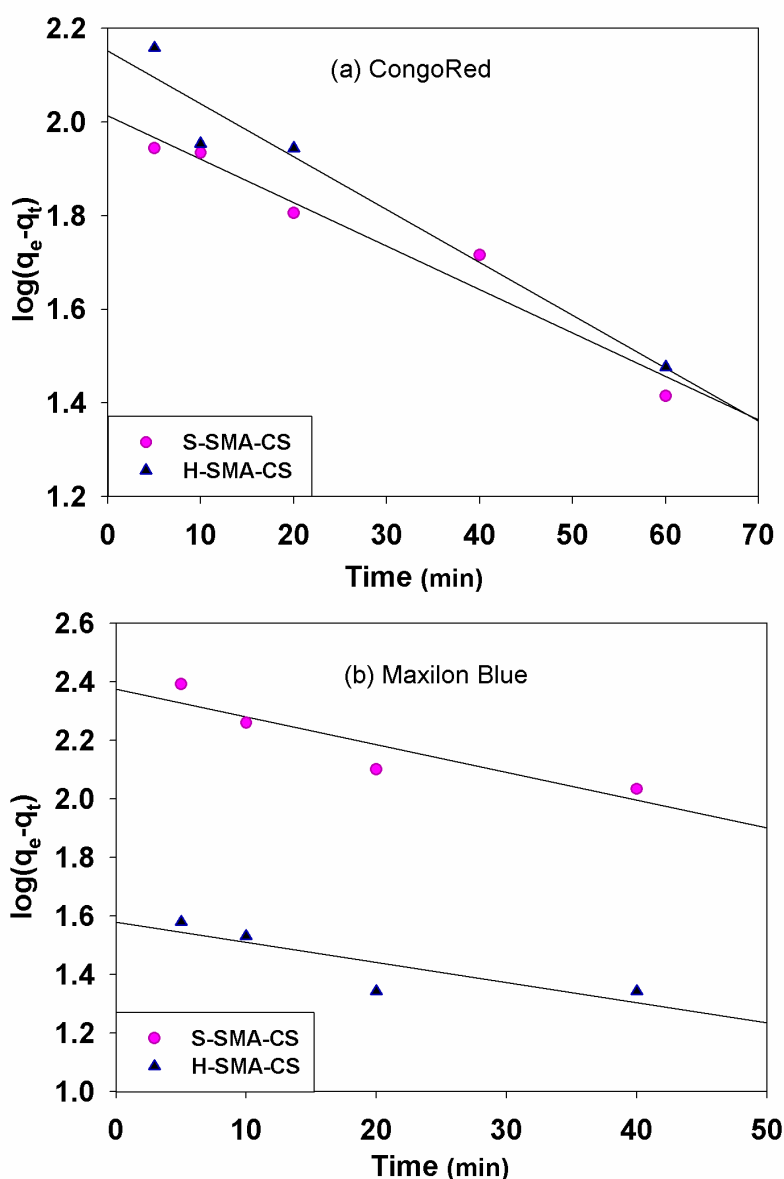


Fig.7 Pseudo-first-order kinetic plots for (a) S-SMA-CS and (b) H-SMA-CS

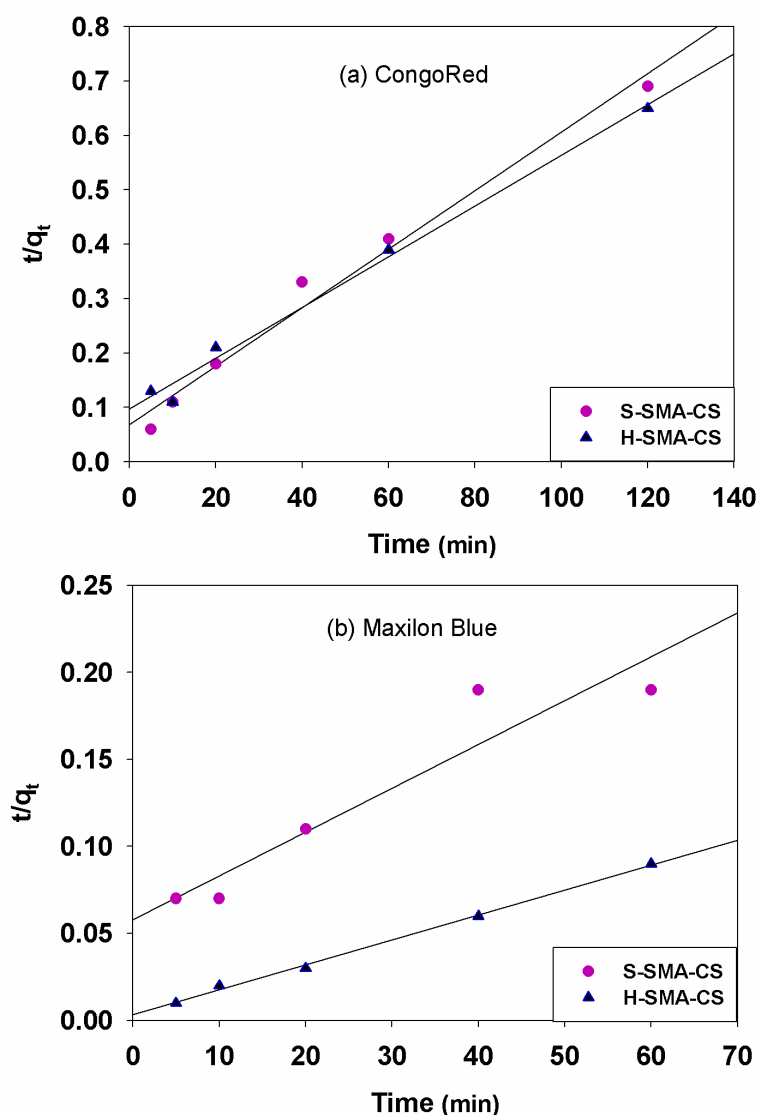


Fig.8. Pseudo-second-order kinetic plots for (a) S-SMA-CS and (b) H-SMA-CS

TABLE 2 Parameters for pseudo-first and pseudo-second order

Dyes	Sample	Pseudo First order			Pseudo Second order		
		q_e	K_1 (min^{-1})	R^2	q_e	K_2 ($\text{g mg}^{-1}\text{min}^{-1}$)	R^2
Congo Red	S-SMA-CS	7.49	0.02	0.96	186.00	0.000425	0.98
	H-SMA-CS	8.59	0.03	0.95	214.00	0.000224	0.99
Maxilon Blue	S-SMA-CS	10.70	0.02	0.83	397.00	0.000111	0.90
	H-SMA-CS	4.84	0.02	0.72	698.00	0.000618	1.00

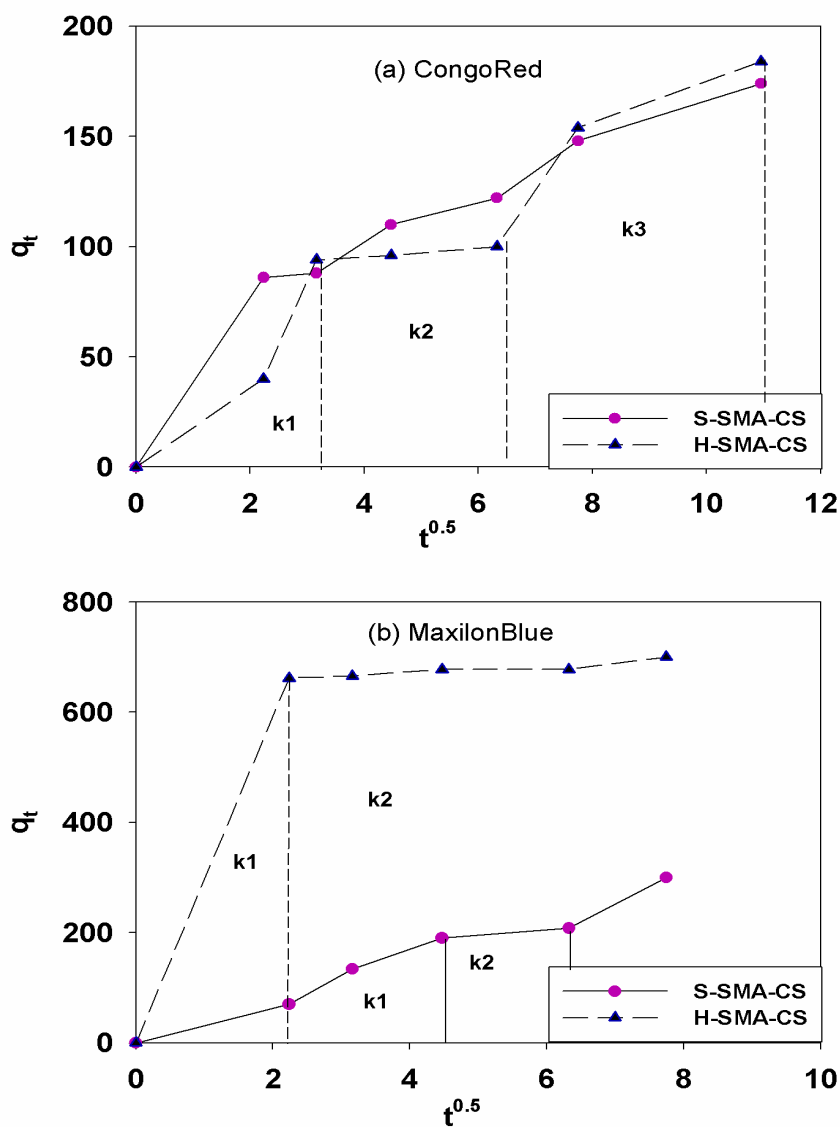


Fig.9 Plots for intra-particle diffusion S-SMA-CS and H-SMA-CS

TABLE 3 . Intra-particle diffusion model constants and correlation coefficients for adsorption of Congo red and Maxilon blue on S-SMA-CS and H- SMA-CS

Dye	Sample	Intra- particle diffusion model			C_1	C_2	C_3	$(R_1)^2$	$(R_2)^2$	$(R_3)^2$
		K_{d1}	K_{d2}	K_{d3}						
Congo Red	S-SMA-CS	38.500	2.160	10.900	0.000	81.200	57.000	1.000	1.000	0.978
	H-SMA-CS	25.800	1.910	16.600	0.000	87.800	7.120	1.000	0.991	0.860
Maxilon Blue	S-SMA-CS	40.900	9.720	---	0.000	147.000	---	1.000	0.981	---
	H-SMA-CS	296.000	6.160	---	0.000	647.000	---	1.000	0.880	---

The results depicted in **Table 3** reveal that the adsorption rate order for Congo red is $k_1 > k_3 > k_2$ adsorption. The obvious sloped line in the first stage epitomizes the boundary layer diffusion, during which Congo red were adsorbed onto the surface of the adsorbent. The second stage began when the adsorption onto the external surface reached saturation, where Congo red adsorbed onto the internal surface. The intra-particle diffusion slows down, causing the occurrence of stage three which is the equilibrium stage, thus the rate limiting step might be internal transfer.

For Maxilon blue intra-particle diffusion plots, exhibited two stages for the two polyelectrolyte complexes. However, the slope of the first stage for H-SMA-CS is much higher than S-SMA-CS, indicating a high external mass transfer at first because of the large surface area and instantaneous feasibility of adsorption active sites. Then, when the saturation was reached, the gradual adsorption stage begun to be considered as the rate-controlling step.

Adsorption isotherm

It is common to use the adsorption isotherm models (Langmuir, and Freundlich) to predict the performance of the adsorbent.

The Freundlich isotherm [47] is an equation based on the assumption that the adsorption process takes place on heterogeneous surfaces and the concentration of the dye at equilibrium has a great role in evaluating the adsorption capacity:

$$q_e = K_F C_e^{1/n} \text{ or } \ln q_e = \ln K_F + \frac{1}{n} \ln C_e \quad (3.8)$$

Where K_F (mg/g (L/mg)^{1/n}) and $1/n$ values are comprehensive evaluation constants of the capacity and the intensity of the adsorption. Usually, a favorable adsorption condition is depicted when values of $n > 1$. The Freundlich isotherm is represented in **Figure 10**.

Equation (3.9) is commonly used to inspect the Langmuir isotherm [47]:

$$\frac{C_e}{q_e} = \left(\frac{1}{Q^0 b}\right) + \left(\frac{1}{Q^0}\right) C_e \quad (3.9)$$

In this equation, q_e stands for the adsorbed weight per weight in grams of sorbent (mg/g), C_e is the equilibrium concentration of the dye in the solution (mg/L), Q^0 is the monolayer adsorption capacity (mg/g) and b is a constant correlated to the adsorption free energy ($b \propto e^{-\Delta G / R}$).

Figure 11 is the Langmuir plot for the two dyes. The Langmuir model deduces the occurrence of a monolayer adsorption. The cause of this behavior is the homogenous of adsorption sites as well as its energies without interactions between the adsorbed dye molecules.

For Congo red the high correlation coefficients ($R^2 > 0.91$) suggest that the equilibrium adsorption data can be well fitted by Freundlich isotherm. The Freundlich model assumes that adsorption occurs on the surface of non-homogeneous medium. This manner is based on the adsorption point and the exponential distribution of energy. As illustrated in **Table 4**, the values of n are greater than one concluding that Congo red is favorably adsorbed by H-SMA-CS and S-SMA-CS.

Maxilon blue equilibrium adsorption data fitted by both model Freundlich and Langmuir for S-SMA-CS. The n value from **Table 4** reflects the favorable adsorption of Maxilon blue onto S-SMA-CS. As the smaller molecular size of Maxilon blue increases, the concentration of dye on the surface increases. In addition, the monovalent nature of Maxilon blue reduces the electrostatic repulsion of the adjacent dye molecule. The value of separation factor R_L indicates the adsorption process as favorable ($0 < R_L < 1$).

However the equilibrium data of adsorption of Maxilon blue onto H-SMA-CS is best fitted to the Freundlich isotherm model with the higher correlation coefficient. Therefore, the adsorption process assumed to be onto the heterogeneous binding sites with different resemblance on the surface of adsorbent. Also, the manifestation of distinct interactions with the dye molecules. As illustrated in **Table 4** the n value is higher than unity. This is a mathematical proof of high adsorption intensity [48].

Conclusion

In this work, two polyelectrolyte complexes based on natural polymer (the extracted chitosan) and two derivatives of the biocompatible polymer (styrene maleic anhydride), have been readily prepared as adsorbents of dyes for wastewater treatment.

- Chitosan was extracted from local shrimp and characterized.
- Styrene maleic anhydride copolymer SMA was prepared, then the two derivatives hydrolyzed and sulphonated SMA were synthesized.

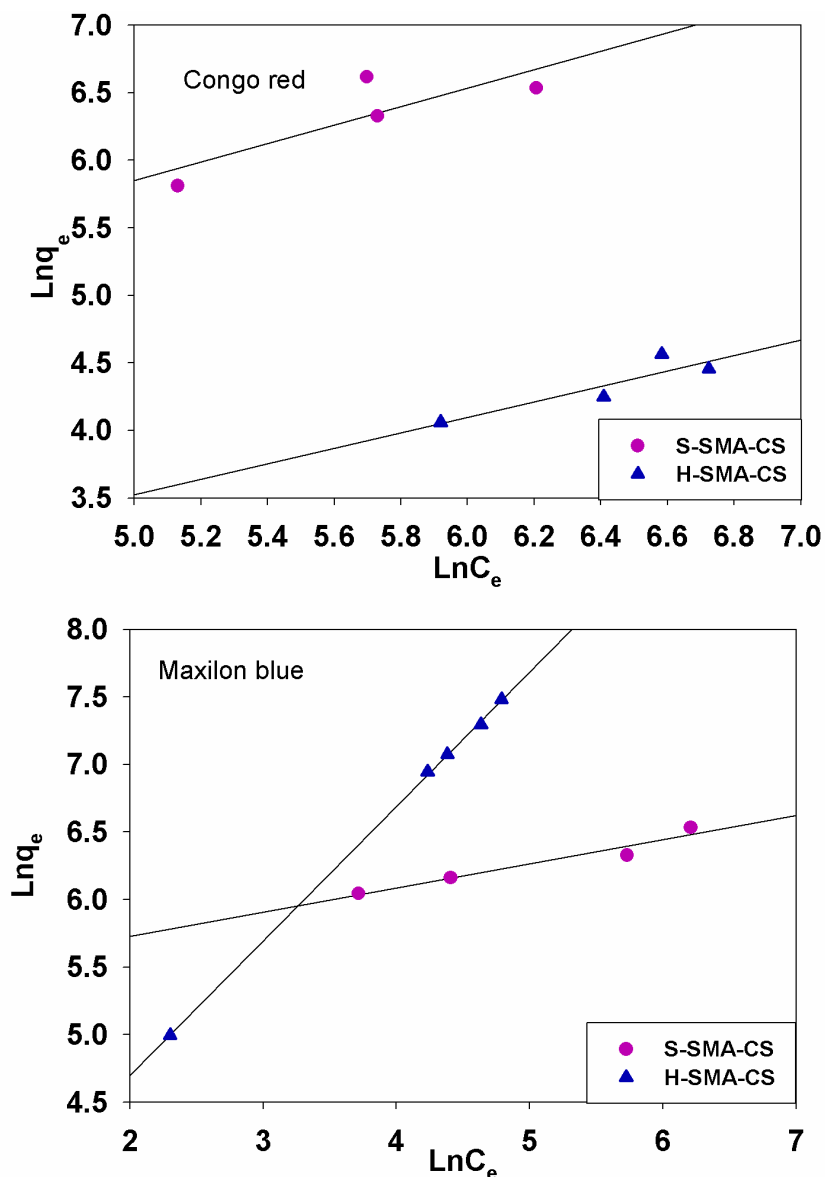


Fig.10. Freundlich isotherm for the adsorption of dyes on S-SMA-CS and H-SMA-CS

TABLE 4 Isotherm model parameters for the adsorption of Congo red and Maxilon blue on S-SMA-CS and H-SMA-CS

Dye	Sample	Langmuir			Freundlich			
		Q_{\max} (mg g^{-1})	K_L (Lmg^{-1})	R^2	R_L	n	K_F	R^2
Congo red	S-SMA-CS	234.00	0.01930	0.87	0.37	0.90	1.14	0.97
	H-SMA-CS	116.00	0.02100	0.88	0.35	1.74	1.92	0.91
Maxilon blue	S-SMA-CS	702.00	0.00004	0.96	1.00	1.13	3.86	0.97
	H-SMA-CS	1830.00	0.00002	0.85	1.00	1.01	14.90	0.92

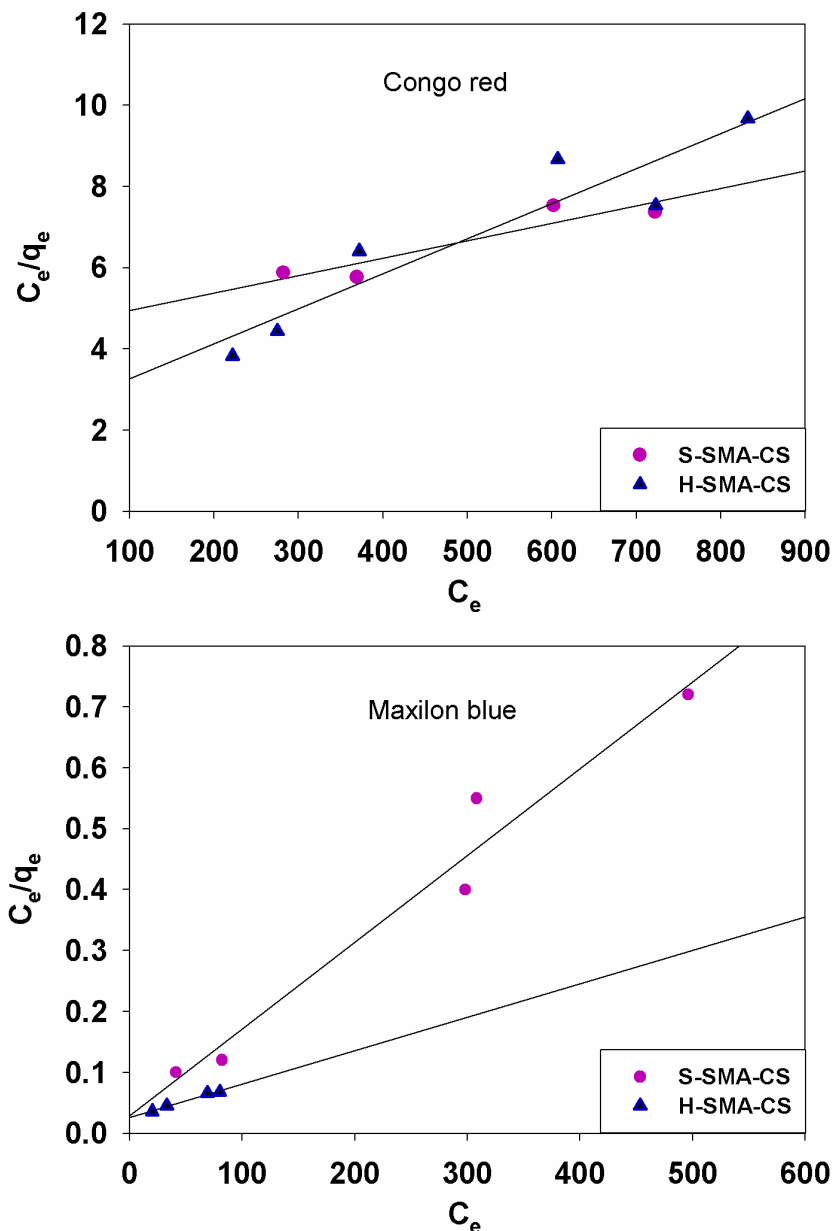


Fig.11 Langmuir isotherm for the adsorption of dyes onto S-SMA-CS and H-SMA-CS

- Two complexes were prepared from chitosan and the two derivatives H-SMA and S-SMA.
- The size of the two complexes H-SMA-CS and S-SMA-CS was determined by (DLS) and they were 423 ± 1 and 100 ± 1 nm, respectively.
- The adsorption capacities of H-SMA-CS and S-SMA-CS for Congo red were 116 and 234 mg/g, respectively. For Congo red, the high correlation coefficients well fitted by

the Freundlich isotherm. Greater than one, n values indicate that Congo red is favorably adsorbed by H-SMA-CS and S-SMA-CS.

- Maxilon blue equilibrium adsorption data fitted by Langmuir for S-SMA-CS. The adsorption capacity was 702 mg/g and the process is favorable as the value of separation factor R_L indicates ($0 < R_L < 1$). However, the Freundlich isotherm is the best fitted model of the adsorption of Maxilon blue onto H-SMA-CS with Q_{max} equal 1830 mg/g.

Acknowledgment

The authors are grateful to the help afforded by Dr. Alena Siskova from Slovakian Polymer Institute for scanning electron microscopy analysis, also for National Research Centre and Cairo University for the provided facilities.

Reference

- Alkan M, Doğan M, Turhan Y, Demirbaş Ö, Turan P: Adsorption kinetics and mechanism of maxilon blue 5G dye on sepiolite from aqueous solutions. *Chem Eng J* 139, 213–223 (2008)
- Yaseen DA, Scholz M: Textile dye wastewater characteristics and constituents of synthetic effluents: a critical review. *Int J Environ Sci Technol* 16, 1193–1226 (2019)
- Ibrahim A, El Fawal GF, Akl MA: Methylene Blue and Crystal Violet Dyes Removal (As A Binary System) from Aqueous Solution Using Local Soil Clay: Kinetics Study and Equilibrium Isotherms. *Egypt J Chem* 62, 541–554 (2019)
- Abdelhamid AE, Elawady MM, El-Ghaffar MAA, Rabie AM, Larsen P, Christensen ML: Surface modification of reverse osmosis membranes with zwitterionic polymer to reduce biofouling. *Water Sci Technol Water Supply* 15, 999–1010 (2015)
- Abdelhamid AE, Khalil AM: Polymeric membranes based on cellulose acetate loaded with candle soot nanoparticles for water desalination. *J Macromol Sci Part A* 56, 153–161 (2019)
- León O, Muñoz-bonilla A, Soto D, Pérez D, Rangel M: Removal of anionic and cationic dyes with bioadsorbent oxidized chitosans. *Carbohydr Polym* 194, 375–383 (2018)
- Gupta VK, Gupta B, Rašogi A, Agarwal S, Nayak A: A comparative investigation on adsorption performances of mesoporous activated carbon prepared from waste rubber tire and activated carbon for a hazardous azo dye-Acid Blue 113. *J Hazard Mater* 186, 891–901 (2011)
- Shaaban AEF, Khalil AAE, Elewa BS, Ismail M, Eldemerdash UM: A New Modified Exfoliated Graphene Oxide for Removal of Copper (II), Lead (II) and Nickel (II) Ions from Aqueous Solutions. *Egypt J Chem* 62, 1823–1849 (2019)
- Sachdeva S, Kumar A: Preparation of nanoporous composite carbon membrane for separation of rhodamine B dye. *J Memb Sci* 329, 2–10 (2009)
- Atia AA, Donia AM, Al-Amrani WA: Adsorption/desorption behavior of acid orange 10 on magnetic silica modified with amine groups. *Chem Eng J* 150, 55–62 (2009)
- Ghaedi M, Biyareh MN, Kokhdan SN, Shamsaldini S, Sahraei R, Daneshfar A, Shahriyar S: Comparison of the efficiency of palladium and silver nanoparticles loaded on activated carbon and zinc oxide nanorods loaded on activated carbon as new adsorbents for removal of Congo red from aqueous solution: Kinetic and isotherm study. *Mater Sci Eng C* 32, 725–734 (2012)
- Ahmadi K, Ghaedi M, Ansari A: Comparison of nickel doped Zinc Sulfide and/or palladium nanoparticle loaded on activated carbon as efficient adsorbents for kinetic and equilibrium study of removal of Congo Red dye. *Spectrochim Acta A Mol Biomol Spectrosc* 136PC, 1441–1449 (2014)
- Mezohegyi G, van der Zee FP, Font J, Fortuny A, Fabregat A: Towards advanced aqueous dye removal processes: A short review on the versatile role of activated carbon. *J Environ Manage* 102, 148–164 (2012)
- Hai FI, Yamamoto K, Fukushi K: Hybrid Treatment Systems for Dye Wastewater. *Crit Rev Environ Sci Technol* 37, 315–377 (2007)
- El-Defrawy MM, Kenawy IMM, ZAKIE, El-tabey RM: Adsorption of the anionic dye (Diamond Fast Brown KE) from textile wastewater onto chitosan/montmorillonite nanocomposites. *Egypt J Chem* (2019)
- Ali EA, Eweis M, Elkholy S, Ismail MN, Elsabee M: The Antimicrobial Behavior of Polyelectrolyte Chitosan-Styrene Maleic Anhydride Nano Composites. *Macromol Res* 26, 418–425 (2018)
- Nada AA, Ali EA, Soliman AAF: Biocompatible chitosan-based hydrogel with tunable mechanical and physical properties formed at body temperature. *Int J Biol Macromol* 131, 624–632 (2019)
- El-Shahat M, Abdelhamid AE, Abdelhameed RM: Capture of iodide from wastewater by effective adsorptive membrane synthesized from MIL-125-NH₂ and Cross-Linked Chitosan. *Carbohydr Polym* 115742 (2019)
- Wan Ngah WS, Teong LC, Hanafiah MAKM: Adsorption of dyes and heavy metal ions by chitosan composites: A review. *Carbohydr Polym* 83, 1446–1456 (2011)

20. Vakili M, Rafatullah M, Salamatinia B, Abdullah AZ, Ibrahim MH, Tan KB, Gholami Z, Amouzgar P: Application of chitosan and its derivatives as adsorbents for dye removal from water and wastewater: A review. *Carbohydr Polym* 113, 115–130 (2014)
21. Zhou L, Jin J, Liu Z, Liang X, Shang C: Adsorption of acid dyes from aqueous solutions by the ethylenediamine-modified magnetic chitosan nanoparticles. *J Hazard Mater* 185, 1045–1052 (2011)
22. Oliveira CS, Airoidi C: Pyridine derivative covalently bonded on chitosan pendant chains for textile dye removal. *Carbohydr Polym* 102, 38–46 (2014)
23. Wang L, Wang A: Adsorption behaviors of Congo red on the N, O-carboxymethyl-chitosan/montmorillonite nanocomposite. *Chem Eng J* 143, 43–50 (2008)
24. Du Q, Sun J, Li Y, Yang X, Wang X, Wang Z, Xia L: Highly enhanced adsorption of congo red onto graphene oxide/chitosan fibers by wet-chemical etching off silica nanoparticles. *Chem Eng J* 245, 99–106 (2014)
25. Abo-baker E, Elkholy SS, Elsabee MZ: Modified Poly (Styrene Maleic Anhydride) Copolymer for the Removal of Toxic Metal Cations from Aqueous Solutions. *Am J Polym Sci* 5, 55–64 (2015)
26. Ali EA, Elkholy SS, Morsi RE, Elsabee MZ: Studies on adsorption behavior of Cu (II) and Cd (II) onto aminothiophene derivatives of Styrene Maleic anhydride copolymer. *J Taiwan Inst Chem Eng* 64, 325–335 (2016)
27. Noor El-Din MR, Morsi RE, Elsabee MZ: Demulsification Efficiency of Some Novel Styrene / Maleic Anhydride Ester Copolymers. *J Appl Polym Sci* 108, 2301–2311 (2008)
28. Öztü C, Küsefoğlu SH: New polymers from plant oil derivatives and styrene-maleic anhydride copolymers. *J Appl Polym Sci* 116, 355–365 (2010)
29. Ignatova M, Stoilova O, Manolova N, Markova N, Rashkov I: Electrospun mats from styrene/maleic anhydride copolymers: Modification with amines and assessment of antimicrobial activity. *Macromol Biosci* 10, 944–954 (2010)
30. Moutinho IMT, Ferreira PJT, Figueiredo ML: Impact of surface sizing on inkjet printing quality. *Ind Eng Chem Res* 46, 6183–6188 (2007)
31. Maeda H: SMANCS and polymer-conjugated macromolecular drugs: Advantages in cancer chemotherapy. *Adv Drug Deliv Rev* 46, 169–185 (2001)
32. Jun S-H, Chang MS, Kim BC, An HJ, Lopez-Ferrer D, Zhao R, Smith RD, Lee S-W, Kim J: Trypsin coatings on electrospun and alcohol-dispersed polymer nanofibers for a trypsin digestion column. *Anal Chem* 82, 7828–34 (2010)
33. Sekhon SS, Park J-M, Ahn J-Y, Park TS, Kwon S-D, Kim Y-C, Min J, Kim Y-H: Immobilization of para-nitrobenzyl esterase-CLEA on electrospun polymer nanofibers for potential use in the synthesis of cephalosporin-derived antibiotics. *Mol Cell Toxicol* 10, 215–221 (2014)
34. Zhang X, Li H, Cao M, Shi L, Chen C: Adsorption of Basic Dyes on β -Cyclodextrin Functionalized Poly (Styrene-Alt-Maleic Anhydride). *Sep Sci Technol* 50, 947–957 (2015)
35. Li Y, Nie W, Chen P, Zhou Y: Preparation and characterization of sulfonated poly (styrene-alt-maleic anhydride) and its selective removal of cationic dyes. *Colloids Surfaces A Physicochem Eng Asp* 499, 46–53 (2016)
36. Eskhan A, Banat F, Selvaraj M, Haija MA: Enhanced removal of methyl violet 6B cationic dye from aqueous solutions using calcium alginate hydrogel grafted with poly (styrene-co-maleic anhydride). *Polym Bull* 1–29 (2018)
37. Buriuli M, Verma D (2017): Polyelectrolyte Complexes (PECs) for Biomedical Applications. In: *Advances in Biomaterials for Biomedical Applications*, Springer, Singapore, Singapore, pp. 45–93
38. Abdou ES, Nagy KSA, Elsabee MZ: Extraction and characterization of chitin and chitosan from local sources. *Bioresour Technol* 99, 1359–1367 (2008)
39. Czechowska-Biskup R, Jarosińska D, Rokita B zen., Ulański P, Rosiak JM: Determination of degree of deacetylation of chitosan-comparison of methods. *Prog Chem Appl Chitin Its Deriv* 17, 5–20 (2012)
40. Jiang X, Chen L, Zhong W: A new linear potentiometric titration method for the determination of deacetylation degree of chitosan. *Carbohydr Polym* 54, 457–463 (2003)
41. Ravindra R, Krovvidi KR, Khan AA: Solubility parameter of chitin and chitosan. *Carbohydr Polym* 36, 121–127 (1998)

42. Lai X, Sun C, Tian H, Zhao W, Gao L: Evaluation of poly(styrene-alt-maleic anhydride)-ethanol as enteric coating material. *Int J Pharm* 352, 66–73 (2008)
43. Vachon D, Cao L, Winek GUS 8,586,637 B2, (2013)
44. Pereira VR, Isloor AM, Bhat UK, Ismail AF: Preparation and antifouling properties of PVDF ultrafiltration membranes with polyaniline (PANI) nanofibers and hydrolysed PSMA (H-PSMA) as additives. *Desalination* 351, 220–227 (2014)
45. Wang W, Bo S, Li S, Qin W: Determination of the Mark-Houwink equation for chitosans with different degrees of deacetylation. *Int J Biol Macromol* 13, 281–285 (1991)
46. Rajput RS, Rupainwar DC, Singh A: A study on styrene maleic anhydride modification by benzoic acid derivatives and dimethyl sulfoxide. *Int J ChemTech Res* 1, 915–919 (2009)
47. Metwally E, Elkholy SS, Salem HAM, Elsabee MZ: Sorption behavior of ^{60}Co and $^{152+154}\text{Eu}$ radionuclides onto chitosan derivatives. *Carbohydr Polym* 76, 622–631 (2009)
48. Vučurović VM, Razmovski RN, Miljić UD, Puškaš VS: Removal of cationic and anionic azo dyes from aqueous solutions by adsorption on maize stem tissue. *J Taiwan Inst Chem Eng* 45, 1700–1708 (2014)

تحضير متراكبات بوليمرية عديدة الشحنة قائمة على الكيتوزان لامتصاص الصبغات الأنيونيه والكاتيونييه

ايمان ابوبكر علي^١، محمد نادر اسماعيل^{٢*}، ماهر زكي السبع^٢

١ قسم البوليمرات والمخضبات، المركز القومي للبحوث، الدقي، جيزه، ١٢٦٢٢ جمهورية مصر العربية
٢ قسم الكيمياء، كلية العلوم، جامعة القاهرة، جيزه ١٢٦١٣ جمهورية مصر العربية

نظرا لما تسببه الكميات الهائلة من الأصباغ الناتجة من العديد من الصناعات من تلوث للمياه اصبح من الضروري إزالة هذه المركبات من النفايات السائلة. تعتبر طريقة الامتزاز ممتازة للتعامل مع كميات كبيرة من الأصباغ دون تشكيل المواد الخطرة. على الرغم من كفاءة تقنية الامتزاز، فإن التكلفة العالية للمواد الممتصة تعتبر حجر عثرة للتطبيقات واسعة النطاق. لذلك تم تحضير مواد ممتزة صديقه للبيئة ومنخفضه التكلفة وفعاله لمعالجة مياه الصرف حيث تم مزج مشتقات البوليمر الثنائي ستيرين مالييك انهيدريد البوليمرات المهدرجة والكبريتية ببوليمر الكيتوزان لتشكل متراكبات متناهية الصغر (النانو) متعددة الشحنة. تم توصيف هيكل وحجم الجسيمات (H-SMA-CS) والسلوك الحراري للمجمعات باستخدام التحليلات الطيفية والحرارية كما تم دراسة استخدام لامتصاص صبغتي الكونغو الأحمر كنموذج للصبغات الأنيونيه والماكسيلون الأزرق كمثال (S-SMA-CS) والصبغات الكاتيونييه ولقد اثبتت النتائج ملائمة طبيعة المواد المحضره للنظام التفاعل ذو الترتيب الثنائي. وكانت قدرات الامتزاز القصوى من الكونغو الحمراء ٢٣٤ و ١١٦ ملغرام/جرام اما بالنسبة للصبغة الماكسيلون الأزرق علي التوالي. كما انها متوافقه H-SMA-CS و S-SMA-CS فقد كانت ٧٠٢ و ١٨٣٠ ملغرام/جرام لكل من لامتصاص Freundlich مع نموذج